

Optimizing Horizontal Manifold Arrangement for Ground Source Heat Pump Using Orthogonal Testing

Cheng Chen^{a,b}, Ruiyong Mao^{a*}, Guoquan Huang^c, Hongwei Wu^d, Zujing Zhang^{a**}

^a College of Civil Engineering, Guizhou University, Guiyang, 550025, China.

^b College of Civil Engineering, Guizhou Provincial Key Laboratory of Rock and Soil Mechanics and Engineering Safety, Guizhou University, Guiyang, 550025, China.

^c AVIC Guizhou Yonghong Radiator Co., Ltd, Guiyang, 550009, China.

^d School of Physic, Engineering and computer science, University of Hertfordshire, Hatfield AL10 9AB, United Kingdom.

*Corresponding author: [tel: +86 139 8505 6628](tel:+8613985056628) email: rymao@gzu.edu.cn.

**Corresponding author: [tel: +86 185 2391 9513](tel:+8618523919513) email: zjzhang3@gzu.edu.cn.

Abstract: This study investigates the importance of improving the heat transfer efficiency of buried pipe systems by optimising the horizontal manifold layout in ground source heat pump systems under summer conditions. Based on the similarity theory, we developed a novel horizontal manifold layout method on a sandbox experimental bench. The heat loss of horizontal manifold in different scenarios (underground garage, lawn, square and road) was investigated by orthogonal tests. The study identifies the optimal layout of the horizontal manifold for different scenarios, with a special focus on how the new layout can effectively reduce the outlet temperature in a 20 °C underground garage environment. The new solution improves the overall heat transfer performance of the system by 37 % compared to the traditional horizontal manifold layout. The study highlights that even if individual component efficiencies are not optimal, a sensible system configuration can still optimise overall performance, and synergies between components need to be considered. Extreme variance analysis reveals the influence of five key factors on the heat transfer efficiency of the horizontal manifold, with surface temperature having the most significant effect. This study provides an integrated optimisation approach for ground source heat pump systems, which is particularly suitable for diverse application scenarios. These findings not only improve the performance of ground source heat pump systems, but also provide valuable guidance for practical engineering design, offering new perspectives on the application and optimisation of ground source heat pump systems.

Keywords: Ground source heat pump; horizontal manifold; Orthogonal experiment; Heat loss; U-shaped heat exchanger.

1.Introduction

Global climate conditions are continuously deteriorating [1, 2], and achieving carbon neutrality has become an imperative goal. In this context, there is a growing demand for heating and cooling buildings using ground source heat pump (GSHP) systems [3]. GSHP systems utilize shallow geothermal heat as a stable and clean energy source [4-6], making a significant contribution to carbon neutrality. For example, in a study conducted by Kapıcıoğlu et al. [7] on the use of GSHP in a 146.5 m² office in a temperate climate zone in Turkey, it was found that GSHP were able to reduce carbon dioxide emissions by 28.9 % and 36.7 % in winter heating compared to the use of a natural gas system and an air source heat pump system, respectively. However, further research is needed to verify whether this result is applicable to other GSHP systems.

A GSHP system consists of three main components: the heat pump unit, U-shaped heat exchanger, and horizontal manifold. Each of these components has a direct impact on the performance and efficiency of the system [8]. Among them, research on the heat pump unit has become increasingly sophisticated. Consequently, in recent years, scholars from various backgrounds have primarily focused their research on two fronts: improving the heat exchange in the U-shaped heat exchanger and reducing heat loss in the horizontal manifold. These efforts aim to enhance the heat exchange efficiency of GSHP systems and lower the initial investment. There are two primary methods for improving heat exchange in the U-shaped heat exchanger: one involves using hybrid systems to mitigate interactions between U-shaped heat exchangers [7, 9-17]. In a study by Zhang et al. [9], the application of a hybrid solar GSHP system in an office building located in Tianjin,

1 China, with a floor area of 4953.4 m², and found that the use of solar energy for heating improved the performance of the
2 system by about 25.8%. While the other focuses on directly enhancing the heat exchange efficiency of the U-shaped heat
3 exchanger by stabilizing the subsurface temperature field [18-24]. Du et al. [21] addressed heat accumulation in the
4 Danjiang City, Jiangsu Province GSHP system demonstration project by developing a numerical model of seepage heat
5 transfer. They adjusted the spacing of heat transfer holes across various zones to a range of 14 m - 21 m, effectively
6 mitigating heat build-up issues and stabilizing the ground temperature field. Both methods can effectively enhance system
7 efficiency, but none of these studies have considered the heat loss in the horizontal manifold.

8 In the current research, there is an obvious gap regarding horizontal manifold heat transfer. Although Tian et al [25]
9 conducted an optimisation study on horizontal manifold, there are some limitations in their experimental design, which
10 makes it difficult to apply their conclusions directly to practical engineering. Specifically, the inlet temperature and surface
11 temperature of the experimental design of Tian et al [25] do not match with the actual engineering environment. At the same
12 time, their experimental design did not fully consider the heat transfer relationship between the piping materials used in the
13 horizontal manifold and the surface covering materials. This makes the gap between the research results and the actual
14 engineering applications, which limits the practicality and universality of the research to a certain extent. Therefore, it is
15 necessary to carry out research that is closer to actual engineering conditions.

16 The aim of this study is to deeply analyse and improve the design and arrangement of horizontal manifold in GSHP
17 systems under summer cooling conditions in order to enhance their practicality and efficiency under different environmental
18 conditions. Therefore, this study builds a 1.5 m × 1.5 m × 1.5 m sand box experimental bench to simulate the actual
19 underground environment based on the similarity theory [26, 27]. Five main factors affecting horizontal manifold were
20 analysed: ground temperature, pipe cover material, pipe burial depth, pipe material and pipe flow rate. These factors are
21 considered to be the key to influence the heat loss of the horizontal manifold and the overall heat transfer efficiency of the
22 system [28-34]. Orthogonal test methods [35-37] were used to explore the specific effects of the above five factors on
23 horizontal manifold heat exchange. By analysing in detail the burial method of horizontal manifold and the key influencing
24 factors in the GSHP system, the heat exchange efficiency and performance of the system in a variety of practical application
25 scenarios were successfully improved. We paid special attention to the common scenarios of horizontal manifold placement
26 under underground garages, lawns, squares and roads [38-42], and adjusted the horizontal manifold placement according to
27 the differences in ground temperatures in these scenarios. With this approach, we not only significantly improved the overall
28 heat-transfer rate and heat transfer efficiency of the system, but also meticulously examined the effects of five factors on the
29 system performance. The innovation of this study is that it not only enhances the effectiveness of individual components,
30 but also emphasises the synergy between components and their adaptability to different environmental conditions, thus
31 significantly improving the practicality and efficiency of GSHP systems in diverse application scenarios. These in-depth
32 discussions and analyses provide new perspectives and practical guidance for the design and optimisation of GSHP systems,
33 and bring important insights for practical engineering applications.

34 **2. Experimental Details**

35 *2.1 Experimental platform*

36 The experimental platform and experimental principles are depicted in Fig. 1. The equipment used to construct the
37 experimental platform comprises a sandbox, a low temperature thermostatic bath, a paperless recorder, a rotameter, a
38 brushless motor pump, a thermostatic water blanket, PT1000 temperature sensors, a computer, and other key components.
39 Photographs of the experimental equipment are presented in Fig. 2, and the primary technical parameters of the equipment
40 are detailed in Table 1.

41 The sand box was set up in the laboratory hall and the experiments were carried out when the ambient temperature of
42 the hall was 23 ± 1 °C. The volume of the sand box was 3.375 m³, which was welded using five pieces of 1.5 m × 1.5 m iron
43 plates as shown in Fig. 1(b). The sand box was covered with 3 cm thick insulation cotton around the sand box to reduce the
44 effect of ambient temperature changes in the hall on the sand box.

45 The sandboxes were backfilled with gravel at a depth of 0 - 1.3 m, with 0 - 1.2 m backfilled with dolomite gravel and

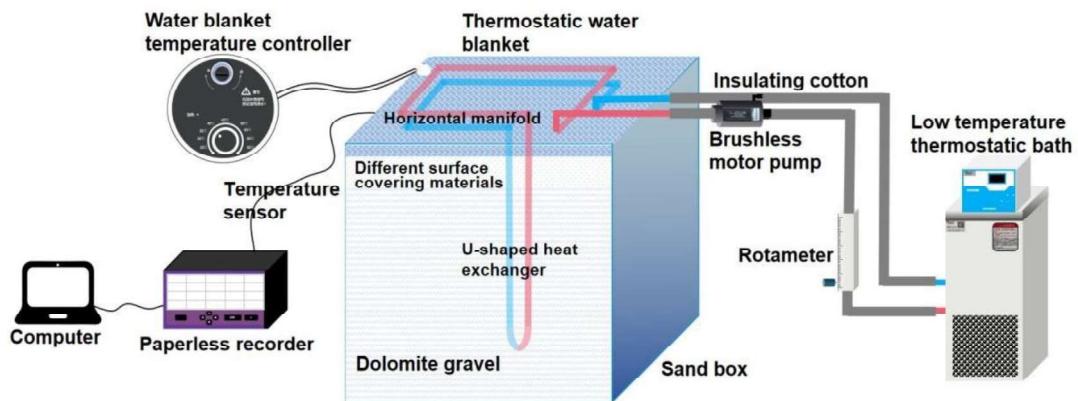
1 1.2 m - 1.3 m backfilled according to the corresponding cover material of the experimental group. (Backfill until the gravel
 2 in the sand box is dry.) The single U-shaped heat exchanger was placed in the centre of the sand box at a depth of 0.1 m -
 3 1.2 m. Its U-shaped pipe had an inner diameter of 9 mm and an outer diameter of 12 mm. The return section of the
 4 horizontal manifold was placed at a depth of 1.22 m, while the water supply section was positioned at a depth of 1.23 m -
 5 1.28 m. Due to space limitations within the sandbox, the horizontal pipe extended around the sandbox for approximately 3/4
 6 of a circle before connecting to the low-temperature constant temperature bath. The length of the horizontal pipe was
 7 approximately 3 m. To achieve the desired operating temperature, a constant temperature water blanket was placed on the
 8 surface of the sandbox gravel, followed by insulation material to elevate the sandbox's gravel surface temperature to the
 9 specified working condition.



(a) Front of the laboratory bench



(b) Lab bench sandbox top



(c) Schematic diagram of the experiment

Fig. 1 Experimental bench and schematic diagram

10 **Table 1** Main technical parameters of the equipment

Installations	Technical Parameters	Types	Manufacturer
Sandbox	1.5 m × 1.5 m × 1.5 m	Self-restraint	-
Low temperature thermostatic bath	Temperature adjustment range: -5 ~ 100 °C	DC-0510	TENLIN
Paperless recorder	36 channels, recording at 3 min intervals	MIK-R600F	MEACON
Rotameter	Flow rate control range: 0.6 ~ 6 L/min; Accuracy: ± 0.216 L/min	FA-15T6L	DARHOR

Brushless motor pump	Flow rate: 17 L/min; head: 28 m	WF40	SURGEFLO
Thermostatic water blanket	Temperature control range: 25 ~ 65 °C	HWM-18F	A.O.SMITH
Temperature sensor	PT1000; Accuracy: $\pm (0.01 + 0.005 t) ^\circ\text{C}$	MIK-WZP	MEACON

1 *2.2 Temperature Sensor Distribution*

2 Temperature sensor 1 is positioned at the initial location of the water supply section of the horizontal manifold.
3 Temperature sensor 2 is placed at the inlet of the U-shaped heat exchanger. Temperature sensor 3 is located at the outlet of the
4 the U-shaped heat exchanger, while temperature sensor 4 is situated at the end of the water return section of the horizontal
5 manifold. To minimize the influence of the gravel surface temperature on the temperature sensors, all sensors are positioned
6 directly beneath the pipelines, as illustrated in Fig. 3. The types and accuracy of the sensors are shown in Table 1. Six
7 temperature measurement points were arranged horizontally at a depth of 1.1 m in the sandbox gravel, and eight temperature
8 measurement points were arranged vertically at a depth of 0.1 m - 1.3 m to detect the range of temperature influence, as
9 shown in Figure 4.



(a)Temperature sensor



(b)Paperless recorder



(c)Rotameter



(d)Brushless motor pump



(e)Thermostatic water blanket



(f)Water blanket temperature controller



(g)Low temperature thermostatic bath



(h)U-shaped heat exchanger

Fig. 2 Diagram of experimental equipment

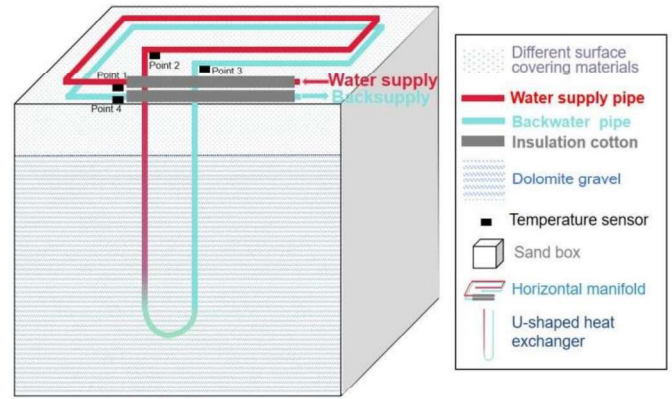
10 *2.3 Initial temperature field of sand box*

11 The experiment was conducted in March, and the initial conditions of the sandbox's horizontal and vertical
12 temperatures are shown in Fig. 5. In Fig. 5(a), it can be observed that as the depth increases, the impact of external factors
13 on the interior of the sandbox gradually diminishes, resulting in a continuous decrease in sandbox temperature. It is also
14 evident that the further the position is from the surface, the more gradual the temperature decrease. The temperature was
15 14.63 °C at a depth of 120 cm from the surface gravel, at which point the surface temperature was 17.82 °C.

16 From Fig. 5(b), it is apparent that at a burial depth of 20 cm, the horizontal temperature within the sandbox remains
17 relatively constant at 16.21 °C. This indicates that at the same depth within the sandbox, the horizontal temperature is
18 essentially uniform.



(a) Layout of temperature measurement points



(b) Schematic layout of temperature measurement points

Fig.3 Arrangement of temperature measurement points of horizontal manifold

1 **2.4 Work Condition Design**

2 To ensure that the experimental findings can be applied to real-world GSHP projects, an experimental platform was
 3 constructed based on similarity theory, with a similarity ratio of 20:1. The primary similarity parameters are outlined in
 4 Table 2.

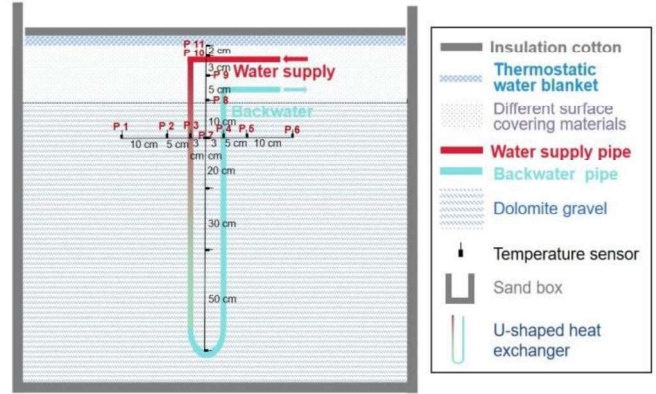
5 **Table 2** Similar design parameters

Parameter type	Original form	Similar model	Similarity multiple
Length of horizontal manifold m	60	3	20:1
Burying depth of return section of horizontal manifold cm	160	8	20:1
Burying depth of water supply section of horizontal manifold cm	40/70/100/130	2.0/3.5/5.0/6.5	20:1
Running time h	400	1	20 ² :1
Reynolds number	4747/7121/9495/11868	4747/7121/9495/11868	1:1
Inlet water temperature °C	30	30	1:1

6 Five influential experimental factors were selected, namely surface temperature, surface covering material, burial depth
 7 of the horizontal manifold water supply section, pipe material, and pipe flow rate. These factors were manipulated to
 8 investigate the heat loss of horizontal manifold under different scenarios. An orthogonal design was used for the experiment
 9 as this method allows the effects of a multi-factor experiment to be systematically arranged and analysed. At the heart of this
 10 design approach is the use of orthogonal arrays to arrange experiments, which ensures that when one factor is examined, the
 11 effects of the other factors are spread evenly. This allows the effects of multiple factors on the results to be effectively
 12 assessed while reducing the number of experiments required. The L16 (4⁵) orthogonal test table was chosen because the
 13 experiment was conducted using 4 levels for each influence factor. The experimental condition design is detailed in Table 3.
 14 Groups 1 - 16 represent experimental groups, with the horizontal manifold buried shallower for the water supply section and
 15 deeper for the return section. Additionally, a control group was designed to mimic actual engineering practices. In the
 16 control group, horizontal manifold were installed using the traditional burial method, with both water supply and return
 17 sections at equal depths. The working conditions of the control group are as follows: a surface temperature of 20 °C,
 18 dolomite gravel as the surface covering material, burial depths of 5.0 cm for both the water supply and return sections,
 19 HDPE as the pipe material, and a pipe flow rate of 3 L/min.

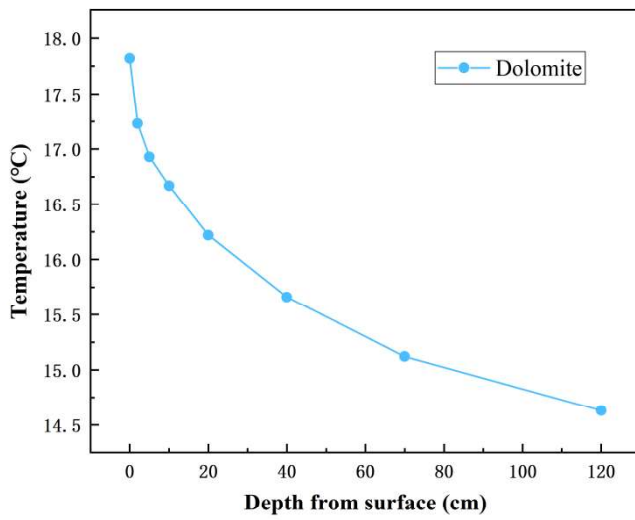


(a) Layout of temperature measurement points

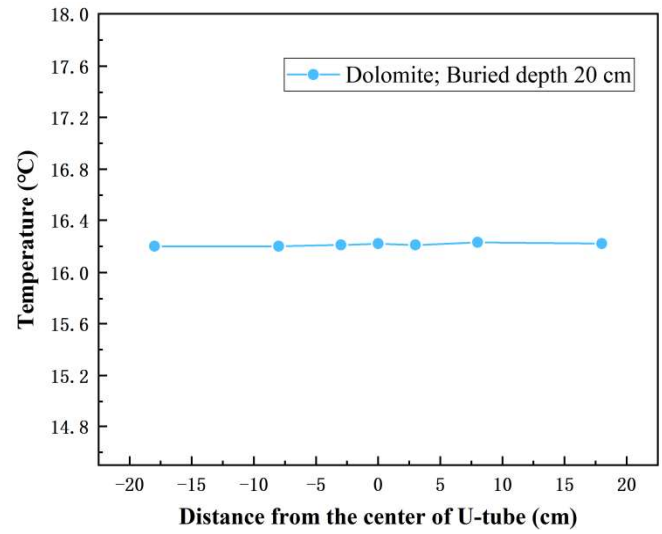


(b) Schematic layout of temperature measurement points

Fig. 4 Arrangement of temperature measurement points inside the sand box



(a) Longitudinal



(b) Transverse

Fig. 5 Initial underground temperature field

1 **Table 3** Orthogonal experimental design

Experimental group	Influential factors				
	Surface temperature °C	Surface cover material	Buried depth of horizontal header section cm	Pipe material	Pipe flow rate L/min
1	20	Dolomite gravel	6.5	PVC	4
2	20	Soil sand	5.0	PE	5
3	20	Limestone gravel	3.5	HDPE	3
4	20	Sandstone gravel	2.0	PA6	2
5	30	Dolomite gravel	5.0	HDPE	2
6	30	Soil sand	6.5	PA6	3
7	30	Limestone gravel	2.0	PVC	5
8	30	Sandstone gravel	3.5	PE	4
9	40	Dolomite gravel	3.5	PA6	5

10	40	Soil sand	2.0	HDPE	4
11	40	Limestone gravel	6.5	PE	2
12	40	Sandstone gravel	5.0	PVC	3
13	50	Dolomite gravel	2.0	PE	3
14	50	Soil sand	3.5	PVC	2
15	50	Limestone gravel	5.0	PA6	4
16	50	Sandstone gravel	6.5	HDPE	5

Through field measurements of different scenarios in three regions of Guizhou Province, the range of surface temperature variations for each scenario can be obtained as shown in Table 4. To facilitate the experiments, the surface temperatures were set at 20 °C, 30 °C, 40 °C and 50 °C. Among them, 20 °C simulates the surface temperature when the horizontal manifold is laid in the underground garage of the building; 30 °C simulates the surface temperature when the horizontal manifold is laid under the lawn; 40 °C simulates the surface temperature when the horizontal manifold is laid under the concrete pavement of the square; and 50 °C simulates the surface temperature when the horizontal manifold is laid under the asphalt pavement. The cover materials on the surface of the horizontal collector pipe were dolomite gravel, soil sand, limestone gravel and sandstone gravel, whose thermal conductivities [25] in the dry state are respectively 2.52 W/(m·K), 1.37 W/(m·K), 3.26 W/(m·K), and 2.78 W/(m·K). Dolomite gravels and limestone gravels range from 5 mm - 10 mm in grain size, sandstone gravels range from 2 mm - 5 mm in grain size, and soil sands range from 0.05 mm - 1 mm in grain size. The burial depth of the horizontal manifold return section remained constant at 8.0 cm, while the water supply section's burial depth was altered to 2.0 cm, 3.5 cm, 5.0 cm, and 6.0 cm. Pipe materials included PE, PVC, PA6, and HDPE, each with distinct thermal conductivities (0.40 W/(m·K), 0.51 W/(m·K), 0.25 W/(m·K), and 0.45 W/(m·K), respectively). Pipe flow rates were set to 2 L/min, 3 L/min, 4 L/min, and 5 L/min.

Table 4 Surface temperature of different scenes in summer

Sites	Longitudes	Longitude	Surface temperature for different scenarios				Climate zone	Measuring time
			Garage (°C)	Lawn (°C)	Plaza (°C)	Asphalt pavement (°C)		
Guiyang	106.67	26.43	18-22	25-31	31-37	42-48	Subtropical monsoon climate	12:00-17:00 (July)
Tongren	109.18	27.73	21-24	31-36	41-45	51-58		
Taijiang	108.41	26.61	18-23	28-34	38-43	48-56		

2.5 Experimental uncertainty

Calculating the uncertainty of the experimental data according to the method proposed by Moffat [43] and Du [44], the relationship between the variable K and the independent variables x_1, x_2, \dots, x_n can be expressed as follows:

$$K = f(x_1, x_2, \dots, x_n)$$

The uncertainty of the variable K is as follows:

$$\sigma_K = \sqrt{\left(\frac{\partial K}{\partial x_1} \sigma x_1\right)^2 + \left(\frac{\partial K}{\partial x_2} \sigma x_2\right)^2 + \dots + \left(\frac{\partial K}{\partial x_n} \sigma x_n\right)^2}$$

Here $\sigma x_1, \sigma x_2, \dots, \sigma x_n$ are the uncertainties of x_1, x_2, \dots, x_n respectively.

Table 5 shows the uncertainties of the measured and calculated parameters.

Table 5 Parameter uncertainty

Item	Units	Uncertainty
Inlet temperature	°C	± 0.01

Outlet temperature	°C	± 0.01
Flow rate	L/min	± 0.216
Temperature difference between inlet and outlet water	°C	± 0.014
Heat-transfer rate	W	± 0.0034

1 *2.6 Experimental steps*

2 The surface temperature of the gravel was adjusted using a temperature-controlled water blanket and thermostat, and
3 pipe flow was regulated by a float flow meter. Subsequently, experiments were conducted by altering the surface covering
4 material, buried pipe depth, and pipe material, as shown in Fig. 6. To ensure the precision of the experimental data, the
5 PT1000 temperature sensor was measured and calibrated prior to the experiment. Additionally, a 3 cm thick layer of
6 insulation cotton was applied to insulate the pipes thermally exposed to the air. After connecting the equipment, initial
7 calibration was performed before proceeding with the experiments.

8 Taking the horizontal manifold as an example of the control group using the traditional buried pipe method, the
9 experimental steps were as follows:

10 (1) Set the temperature of the cryostat tank to 30 °C, ensuring that the temperature of the inlet pipe of the horizontal
11 manifold was 30 °C

12 (2) Uniformly arrange 6 PT1000 temperature sensors on the gravel surface to measure the surface temperature of the
13 gravel. Place the temperature-controlled water blanket over the upper part of the PT1000 temperature sensors, while
14 covering the surface of the water blanket with insulation cotton to prevent heat dissipation.

15 (3) Use the temperature-controlled water blanket thermostat to raise the displayed temperature of the PT1000
16 temperature sensors located on the gravel surface to 20 °C

17 (4) Set the recording interval of the paperless recorder to 3 minutes for data recording.

18 (5) Activate the brushless motor pump and adjust the float flow meter to maintain a flow rate of 3 L/min.

19 (6) After running for 1 hour, shut down the system.

20 (7) Utilize a computer to process and analyze the temperature data recorded by the paperless recorder.

21 The experimental steps for experimental groups 1-16 were the same as those for the control group, all of which were to
22 shut down the system after 1 hour of operation. In order to eliminate as much as possible the effect of the previous set of
23 experiments on the temperature of the sand box, and at the same time the next set of experiments to replace the piping
24 material, the surface covering material and the horizontal collector water supply section of the burial depth of the time
25 required, so the next set of experiments carried out in about 24 hours after the next set of experiments.



(a) 20 °C sandstone PA6

(b) 30 °C dolomite HDPE

(c) 40 °C limestone PE

(d) 50 °C soil PVC

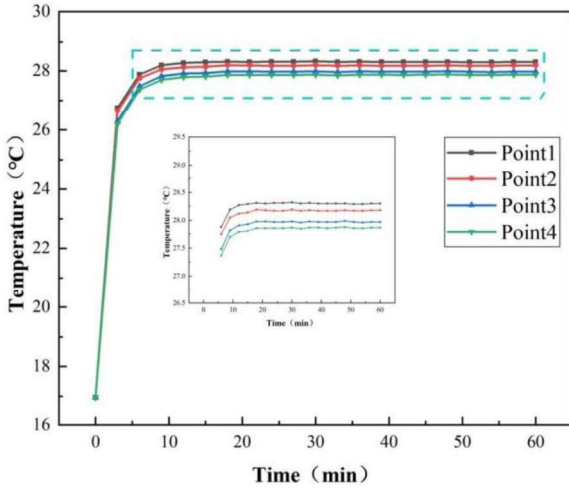
Fig. 6 Buried pipes in the water supply section at different surface temperatures

1 **3. Experimental results and analysis**

2 *3.1 Analysis of temperature change of horizontal manifold under different working conditions*

3 **3.1.1 Temperature changes under initial operating conditions**

4 The control group is the initial working condition, and the system's operating parameters are as follows: the water
 5 supply and return sections of the horizontal manifold are both buried at a depth of 5.0 cm, the surface temperature is 20 °C,
 6 the surface covering material is dolomite gravel, the pipe material is HDPE, and the pipe flow rate is 3 L/min. After running
 7 the system for 1 hour, the temperature changes of the sensors placed in the water supply and return sections of the horizontal
 8 manifold are illustrated in Fig. 7.



9 **Fig. 7** Variation of horizontal manifold temperature
 10 sensor under initial operating conditions

11 From Fig. 7, it can be seen that the temperatures of the
 12 four sensors gradually equilibrated after the experiment was
 13 run for about 10 min. And in 1h, the sensor temperatures no
 14 longer change. At this time, the temperatures of point 1,
 15 point 2, point 3, and point 4 increased from 16.96 °C,
 16 16.96 °C, 16.96 °C, 16.96 °C to 28.30 °C, 28.18 °C, 27.97 °C,
 17 and 27.87 °C, respectively. After the experimental run
 18 reached a steady state, the temperatures from temperature
 19 sensor 1 to temperature sensor 2 (water supply section of the
 20 horizontal manifold), temperature sensor 2 to temperature
 21 sensor 3 (U-type heat exchanger section), and temperature
 22 sensor 3 to temperature sensor 4 (return section of the
 23 horizontal manifold) decreased by 0.12 °C, 0.21 °C, and
 24 0.10 °C, respectively. This is because the inlet temperature of
 25 the pipe is set to 30 °C, and the temperature of the
 geotechnical body is lower than that of the pipe, and the heat

26 exchange between the geotechnical body and the pipe results in a lower temperature of the pipe. Although the water supply
 27 section and water return section have the same burial depth, the reduced temperature of the water supply section is 0.02 °C
 28 higher than that of the water return section because the water inlet temperature of the water return section is not as high as
 29 the water inlet temperature of the water supply section. The overall heat exchange of the control system was 84.3 W.

30 **3.1.2 Temperature change at 20 °C surface temperature**

31 The burial depth of the horizontal manifold return section in experimental groups 1 - 16 was kept constant at 8.0 cm.
 32 According to Table 3 to change the surface temperature, water supply section burial depth, surface covering materials, pipe
 33 materials and pipe flow rate for the experiment, the experimental run within 12 minutes, four sensors temperature rises
 34 sharply, and then reached stability. The temperature of the horizontal collector pipe after stabilisation is shown in Table 6,
 35 where the supply indicates the temperature change in the water supply section from point 1 to point 2, the U-pipe indicates
 36 the temperature change from point 2 to point 3, and return indicates the temperature change in the return section from point
 37 3 to point 4.

38 **Table 6** Temperatures at horizontal header measurement points

Temp (°C)	Experimental group															
	1	2	3	4	5	6	7	8	9	10	11	12	13	14	15	16
Point 1	28.24	28.31	28.32	28.33	28.27	28.35	28.66	28.46	28.84	28.92	28.29	28.33	30.27	29.86	29.34	29.07
Point 2	28.01	28.21	28.16	28.21	28.35	28.29	28.90	28.60	28.99	29.14	28.35	28.45	30.65	30.04	29.55	29.22
Point 3	27.83	28.01	27.97	28.01	28.13	28.10	28.62	28.37	28.74	28.87	28.14	28.23	30.33	29.80	29.29	28.99

Point 4	27.65	27.90	27.79	27.87	28.00	28.00	28.39	28.27	28.77	28.76	28.19	28.30	30.45	29.87	29.42	29.12
Supply	-0.23	-0.10	-0.16	-0.12	0.08	-0.06	0.24	0.14	0.15	0.22	0.06	0.12	0.38	0.18	0.21	0.15
U-tube	-0.18	-0.20	-0.19	-0.20	-0.22	-0.20	-0.28	-0.23	-0.25	-0.27	-0.21	-0.22	-0.32	-0.24	-0.26	-0.23
Return	-0.18	-0.11	-0.18	-0.14	-0.13	-0.09	-0.23	-0.10	0.03	-0.11	0.05	0.07	0.12	0.07	0.13	0.13

At a surface temperature of 20 °C, the temperature change of the four sensors after changing the factors in experimental groups 1 - 4 is shown in Fig. 8. In Fig. 8(a), the temperatures at points 1, 2, 3, and 4 increased from 16.89 °C, 16.89 °C, 16.84 °C, and 16.84 °C to column 2 of Table 6.

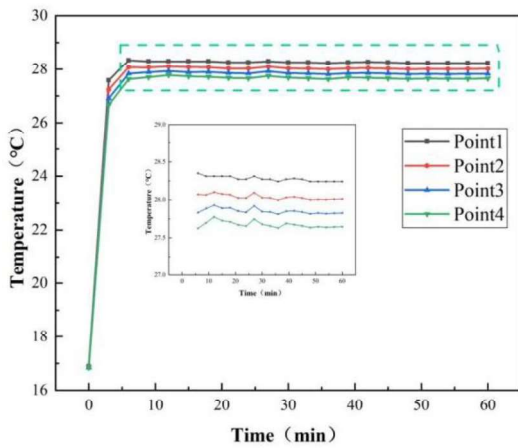
Since the ground temperature of 20 °C is lower than the pipeline's set inlet temperature, both the water supply and return sections of the horizontal manifold exhibited an exothermic state, with heat from the pipeline being absorbed by the surface covering material. The water supply section, with a burial depth of 6.5 cm in gravel, had lower temperatures, and the PVC pipe material, with higher thermal conductivity, facilitated more efficient heat exchange with the covering material, resulting in a more significant temperature decrease of 0.23 °C in the water supply section. Conversely, the return section, buried 1.5 cm deeper than the water supply section, did not experience as much temperature reduction because of its lower inlet temperature and the influence of heat accumulation from the water supply section on the covering material. The temperature decrease in the return section was only 0.18 °C. The U-shaped heat exchanger contributed to temperature reduction by exchanging heat with the geotechnical body inside the sandbox.

Compared to the control group, Experimental Group 1, with the same ground temperature and covering material, can improve the overall system heat transfer by 12.5 W by altering the buried pipe arrangement, pipe material, and pipe flow rate. From the comparison, it is evident that after 1 hour of operation, Experimental Group 1 carries away 0.11 °C more heat in the water supply section compared to the initial condition, while the return section carries away 0.08 °C more heat. The increased heat dissipation in the water supply section of Experimental Group 1 is attributed not only to the deeper burial depth but also to the higher thermal conductivity of PVC compared to HDPE. However, the U-shaped heat exchanger in Experimental Group 1 removes 0.03 °C less heat from the geotechnical body.

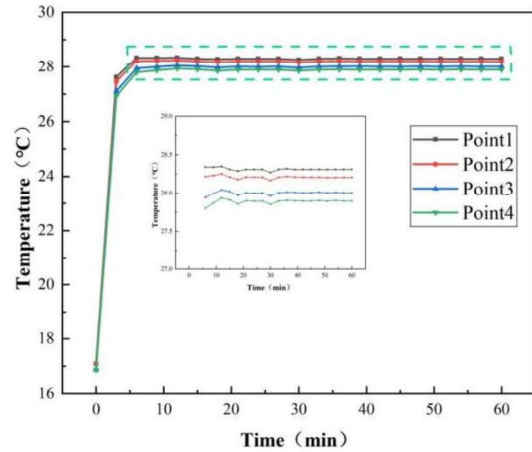
As depicted in Fig. 8(b), temperatures at points 1, 2, 3, and 4 rise from their initial values of 17.08 °C, 17.08 °C, 16.87 °C, and 16.87 °C to column 3 of Table 6. Comparing with Experimental Group 1, Experimental Group 2 experienced a reduction of 0.13 °C in heat dissipation from the water supply section and a decrease of 0.07 °C in the return section, despite only reducing the burial depth by 1.5 cm. However, the heat carried away by the U-shaped heat exchanger increased by 0.02 °C. When the ground temperature was 20 °C, Experimental Group 2 had the least amount of heat dissipation from both the water supply and return sections due to the covering material's low thermal conductivity. This low thermal conductivity effectively prevented heat loss, resulting in heat buildup, which was not conducive to heat exchange between the pipeline and the surrounding geotechnical body. Moreover, the higher pipeline flow rate in this group led to a faster flow velocity, causing the fluid to return to the thermostat tank before complete heat exchange with the covering material. Additionally, the pipeline material, PE, had a low thermal conductivity, which also had an impact on the pipe's heat dissipation to some extent.

As shown in Fig. 8(c), the temperatures at points 1, 2, 3, and 4 increased from 17.17 °C, 17.17 °C, 16.82 °C, and 16.82 °C to column 4 of Table 6. Compared to Experimental Group 2, Experimental Group 3 had a shallower burial depth, and under normal circumstances, the reduction in temperature of the water supply section should have been lower than that of Experimental Group 2. However, due to the fact that the covering material, limestone, had the highest thermal conductivity, and at the same time, the pipe material, HDPE, also had a higher thermal conductivity, the reduction in temperature in both the water supply section and the water return section was actually 0.06 °C and 0.07 °C higher than in Experimental Group 2. The reduction in temperature in the water return section of Experimental Group 3 was the same as that in Experimental Group 1, both being 0.18 °C. It can be observed that this was due to the identical burial depth of the horizontal manifold return section. Although limestone had higher thermal conductivity than dolomite, the pipe material HDPE had lower thermal conductivity than PVC. Additionally, the flow rate in Experimental Group 3 was lower than that in Experimental

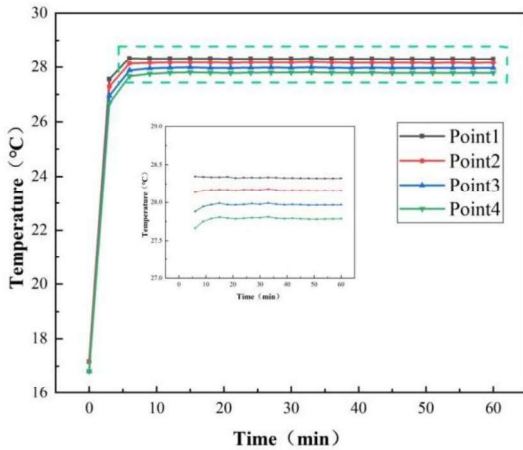
1 Group 1, and the combined influence of these three factors resulted in the same reduction in temperature in the return
 2 section for both groups.



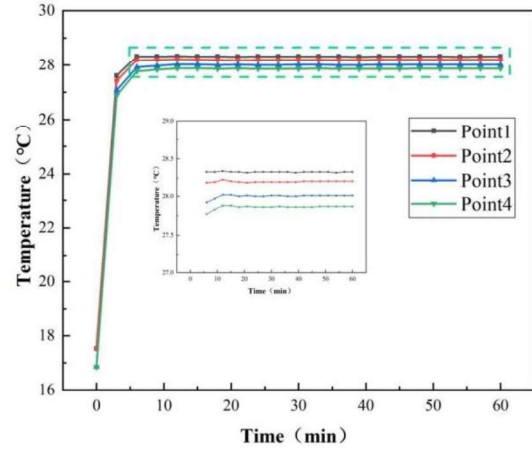
(a) Group 1: dolomite gravel, 6.5 cm, PVC, 4L/min



(b) Group 2: soil sand, 5.0 cm, PE, 5 L/min



(c) Group 3: limestone gravel, 3.5 cm, HDPE, 3 L/min



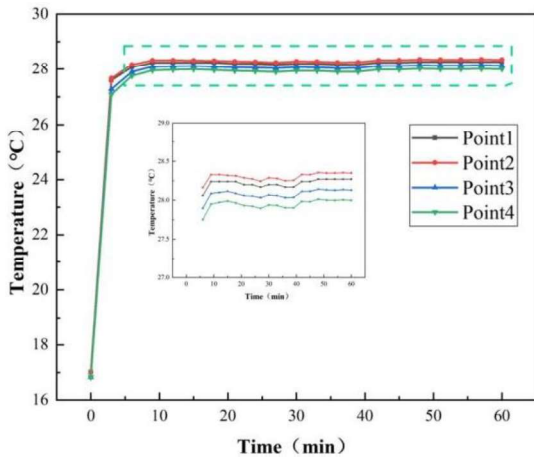
(d) Group 4: sandstone gravel, 2.0 cm, PA6, 2 L/min

Fig. 8 Horizontal manifold Temperature Sensor Change at 20 °C Surface Temperature

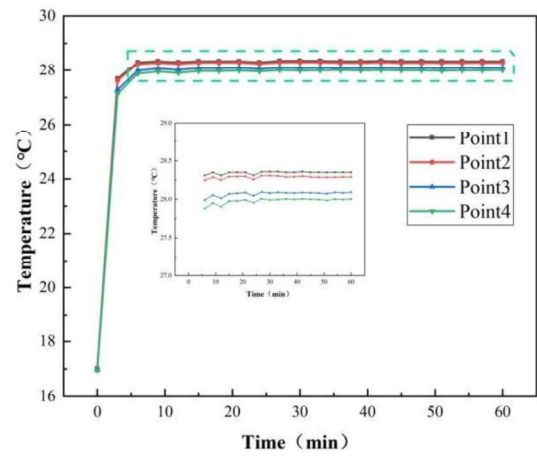
3 As shown in Fig. 8(d), the temperatures at points 1, 2, 3, and 4 increased from 17.52°C, 17.52°C, 16.85°C and 16.85°C to
 4 column 5 of Table 6. Comparing with Experimental Group 3, Experimental Group 4 had a temperature reduction in both the
 5 water supply section and the return section that was 0.04°C lower. This was due to the fact that the water supply section of
 6 Experimental Group 4 had the shallowest burial depth, the pipe material was PA6 with the lowest thermal conductivity, and
 7 the covering material, sandstone, also had a lower thermal conductivity than limestone, resulting in a smaller reduction in
 8 temperature.

9 3.1.3 Temperature change at 30 °C surface temperature

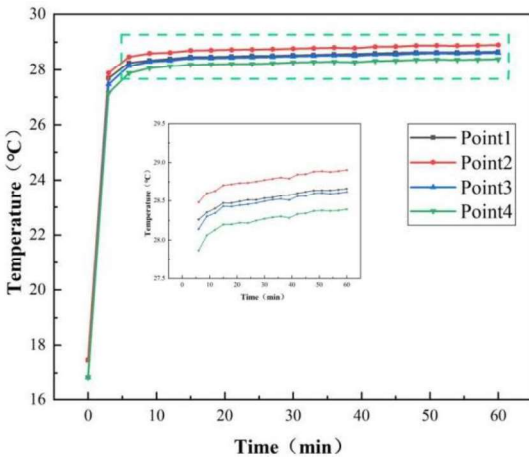
10 When the surface temperature is 30 °C, the temperature change of the four sensors after changing the factors in the
 11 experimental group 5 - 8 is shown in Fig. 9. Compared to the first four groups of experiments, in Experimental Groups 5, 7,
 12 and 8, the water supply section of the horizontal manifold no longer exhibited a temperature reduction; instead, it showed an
 13 increase in temperature. While in Experimental Group 6, although the water supply section still demonstrated a temperature
 14 decrease, the decrease was not significant, only 0.06 °C. It can be inferred that the temperature increase in the water supply
 15 section is attributed to heat absorption from the covering material.



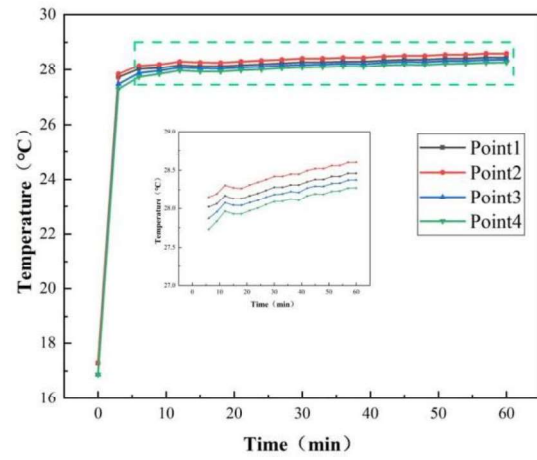
(a) Group 5: dolomite gravel, 5.0 cm, HDPE, 2L/min



(b) Group 6: soil sand, 6.5 cm, PA6, 3 L/min



(c) Group 7: limestone gravel, 2.0 cm, PVC, 5L/min



(d) Group 8: sandstone gravel, 2.0 cm, PE, 4 L/min

Fig. 9 Horizontal manifold Temperature Sensor Change at 30 °C Surface Temperature

1 As shown in Fig. 9(a), the temperatures at points 1, 2, 3, and 4 increased from 17.01 °C, 17.01 °C, 16.83 °C, and 16.83 °C
 2 to column 6 of Table 6. When the ground temperature was 30 °C, the surface covering material dolomite was heated, and heat
 3 was transferred downward, increasing the temperature of the water supply section. Since the water supply section of
 4 experimental group 5 was buried at a depth of 5.0 cm, it was less influenced by the ground temperature, resulting in only a
 5 0.08 °C temperature increase. The return water section, buried at a depth of 8.0 cm, was not affected by the ground
 6 temperature and continued to exhibit a temperature decrease.

7 As shown in Fig. 9(b), the temperatures at points 1, 2, 3, and 4 increased from 17.02 °C, 17.02 °C, 16.96 °C, and 16.96 °C
 8 to column 7 of Table 6. Compared to Experimental Group 5, the water supply section in Experimental Group 6 exhibited a
 9 lower temperature decrease. This is attributed to Experimental Group 6 having a 1.5 cm deeper burial depth in the water
 10 supply section, coupled with the use of soil with the lowest thermal conductivity as the covering material and PA6 with the
 11 lowest thermal conductivity as the pipe material. It's the minimal thermal conductivity of both the covering material and
 12 pipe material that leads to reduced heat being carried away from the pipe by the covering material, resulting in a lower
 13 temperature decrease in the return water section compared to Experimental Group 5. It can be inferred that the lower flow
 14 rate enhances heat exchange between the pipe and the covering material, although it is not the most critical factor
 15 influencing heat exchange.

16 As depicted in Fig. 9(c), over 1 hour of operation, the temperatures at points 1, 2, 3, and 4 increased from 17.46 °C,
 17 17.46 °C, 18.64 °C, and 18.64 °C to column 8 of Table 6. At a ground temperature of 30 °C, Experimental Group 7 showed the
 18 most significant temperature variations in both the water supply section and return section of the horizontal manifold. This
 19 is because the surface covering material, limestone, and the pipe material, PVC, have the highest thermal conductivity,

1 which effectively dissipates heat from the pipe and results in the largest temperature difference. Additionally, the water
2 supply section is buried at the shallowest depth, making it considerably influenced by ground temperature.

3 As depicted in Fig. 9(d), the temperatures at points 1, 2, 3, and 4 increased from 17.28 °C, 17.28 °C, 16.87 °C, and 16.87 °C
4 to column 9 of Table 6. When compared to Experimental Group 7, Experimental Group 8 demonstrated a 0.13 °C lower
5 temperature reduction in the return section despite having the same burial depth for the return section. This difference can be
6 attributed to the enhanced heat exchange properties of the covering material and pipe material used in Experimental Group 7.
7 Even though Experimental Group 8 had a lower pipe flow rate, it's important to note that pipe flow rate is not the most
8 critical factor influencing heat exchange. Furthermore, the water supply section in Experimental Group 8 was buried deeper
9 than in Experimental Group 7, and the lower thermal conductivity of sandstone and PE had a suppressing effect on pipe heat
10 exchange. Consequently, the temperature increase in the water supply section of Experimental Group 8 was 0.10 °C lower
11 than that of Experimental Group 7.

12 **3.1.4 Temperature change at 40 °C surface temperature**

13 When the surface temperature is 40 °C, the experimental group 9 - 12 changed the factors and the temperature change
14 of the four sensors is shown in Fig. 10. It can be observed that the water supply section temperatures increased in all four
15 experimental groups. The water return section temperature decreased in Experimental Group 10, while it increased in
16 Experimental Groups 9, 11, and 12. As the water supply section burial depth increased, the temperature rise in the water
17 supply section decreased. Although the burial depth of the water return section was the same, the temperature changes in the
18 water return section varied due to differences in covering materials, pipe materials, and pipe flow rates. Additionally, due to
19 the increase in surface temperature, there was a delay in heat transfer through the covering material, and it can be found that
20 the temperature of the pipes no longer changed rapidly until after 12 minutes.

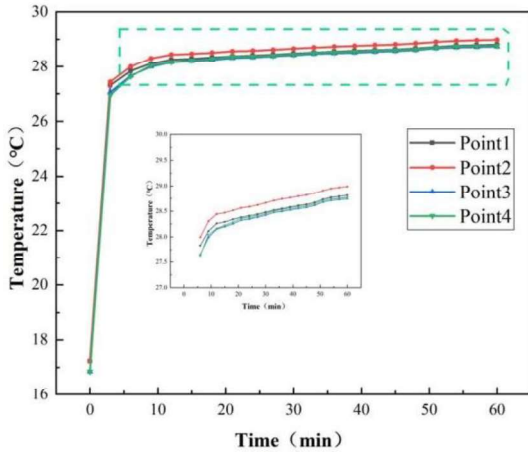
21 As shown in Fig. 10(a), the temperatures at points 1, 2, 3, and 4 increased from 17.23 °C, 17.23 °C, 16.85 °C, and 16.85 °C
22 to column 10 of Table 6. The temperature increased sharply before 12 minutes and then exhibited a slower rise. When the
23 surface temperature is 40 °C, the temperature of the water supply section increases because it is shallowly buried and the
24 surface covering material, dolomite, does not have the lowest thermal conductivity. However, the pipe material, PA6, has the
25 lowest thermal conductivity, and the pipe flow rate is the highest, which is not conducive to heat exchange between the pipe
26 and the covering material. Therefore, the temperature rise in the water supply section is not the highest.

27 As shown in Fig. 10(b), the temperatures at points 1, 2, 3, and 4 increased from 17.55 °C, 17.55 °C, 16.86 °C, and 16.86 °C
28 to column 11 of Table 6. The return section temperature decreases in the water supply section of Experimental Group 10,
29 even though it has the highest temperature rise. Compared to Experimental Group 9, both have the same return section
30 burial depth, but the return section temperature decreases in Experimental Group 10 due to the fact that the surface covering
31 material in Experimental Group 10 is soil with the lowest thermal conductivity, which significantly reduces the influence of
32 surface temperature on the return section. It can be observed that in Experimental Group 9, the pipe material, despite having
33 lower thermal conductivity and higher pipe flow rate, increases the temperature of the return section, indicating that the
34 surface covering material has a greater impact on the temperature changes in the water supply and return sections than the
35 pipe material and pipe flow rate.

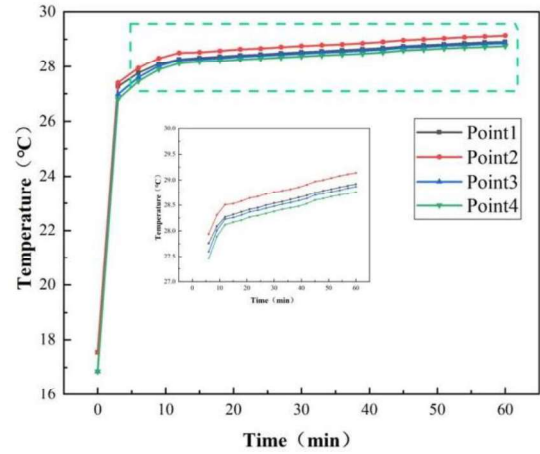
36 As shown in Fig. 10(c), after running for 1 hour, the temperature increased from 16.87 °C, 16.87 °C, 16.83 °C, and 16.83 °C
37 to column 12 of Table 6. The difference in burial depth between the water supply section and the return section in
38 Experimental Group 11 is only 1.5 cm, so the temperature rise is nearly identical. Compared to Experimental Group 10,
39 under the same burial depth, the temperature rise in the water return section in Experimental Group 11 is due to the higher
40 thermal conductivity of the surface covering material, tuff, which facilitates the downward transfer of ground temperature. It
41 can be observed that when the ground temperature reaches 40 °C, even with a water supply section buried at a depth of 6.5
42 cm, the water supply section is still affected by the ground temperature.

43 As shown in Fig. 10(d), the temperatures at point 1, point 2, point 3, and point 4 increased from 17.16 °C, 17.16 °C,
44 16.91 °C, and 16.91 °C to column 13 of Table 6. The temperature changes mainly occurred within the first 12 minutes, and
45 the temperature rise became less significant after 12 minutes. With a surface temperature of 40 °C, under the same burial

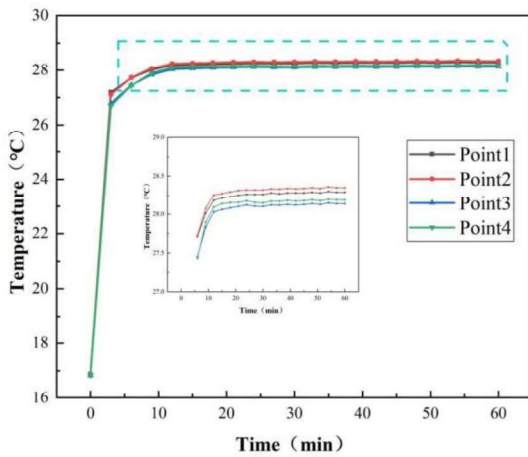
1 depth in the return section, Experimental Group 12 had the highest temperature rise in the return section due to the fact that
 2 the pipe material PVC has the highest thermal conductivity. Comparing it with Experimental Groups 9, 10, and 11, it can be
 3 concluded that an increase in the water supply section temperature improves the heat-transfer rate of the U-shaped heat
 4 exchanger. This is because the higher inlet temperature of the U-shaped heat exchanger leads to a greater temperature
 5 difference between the pipe and the surrounding geotechnical body, thus enhancing heat exchange.



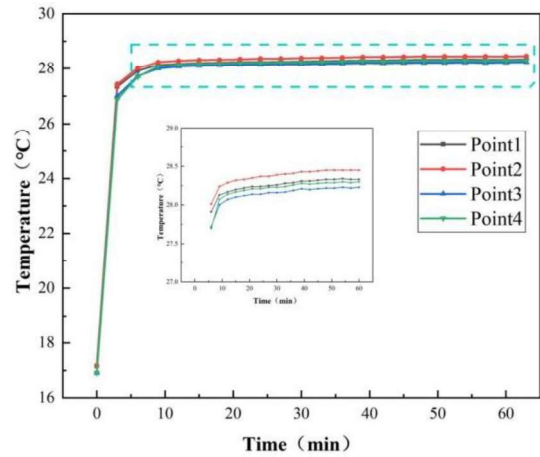
(a) Group 9: dolomite gravel, 3.5 cm, PA6, 5 L/min



(b) Group 10: soil sand, 2.0 cm, HDPE, 4 L/min



(c) Group 11: limestone gravel, 6.5 cm, PE, 2 L/min



(d) Group 12: sandstone gravel, 5.0 cm, PVC, 3 L/min

Fig. 10 Horizontal manifold Temperature Sensor Change at 40 °C Surface Temperature

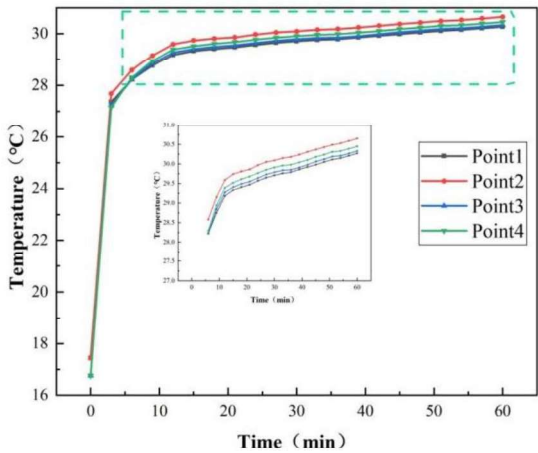
6 3.1.5 Temperature change at 50 °C surface temperature

7 When the surface temperature is 50 °C, all four experimental groups show an increase in temperature in both the water
 8 supply and return sections, as depicted in Fig. 11. Due to the rising surface temperature, during the 1hour experiment, it can
 9 be observed that the pipe temperatures undergo rapid changes within the first 12 minutes, followed by a gradual increase in
 10 temperature after the 12 minutes mark. Additionally, this upward trend becomes progressively less steep as the burial depth
 11 increases.

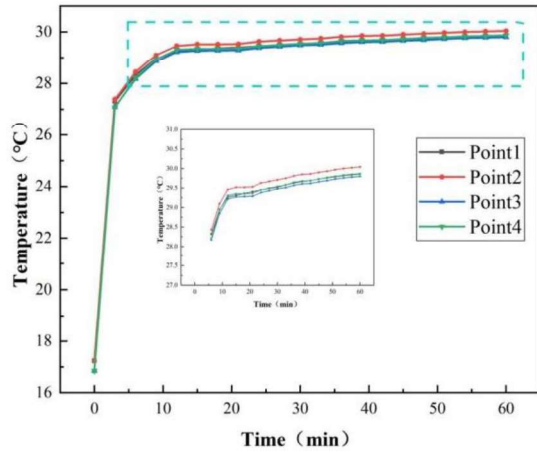
12 As shown in Fig. 11(a), at points 1, 2, 3, and 4, the temperatures increase from 17.44 °C, 17.44 °C, 16.77 °C, and 16.77 °C
 13 to column 14 of Table 6. Experimental Group 13 exhibits the highest temperature increase in the water supply section. It can
 14 be noted that when the burial depth is at its shallowest, the ground temperature has a significant impact on the heat exchange
 15 between the water supply section and the surface covering material. Furthermore, due to the elevated surface temperature,
 16 even with increased burial depth, the use of slightly more thermally conductive covering and piping materials can result in
 17 an increase in the return section's temperature. Although the increased temperature in the water supply section enhances heat
 18 exchange in the U-type heat exchanger, it leads to greater overall heat loss for the system.

1 As shown in Fig. 11(b), the temperatures at points 1, 2, 3, and 4 increased from 17.23 °C, 17.23 °C, 16.85 °C, and 16.85 °C
 2 to column 15 of Table 6. The temperature rises sharply by 12 minutes, and there is still a temperature rise at 12 minutes, but
 3 the trend of increase is relatively flat. Compared to Experimental Group 13, the water supply section's temperature rise was
 4 lower in Experimental Group 14 due to the minimum thermal conductivity of the soil surface cover material as well as the
 5 increased burial depth. When the surface temperature was the same, Experimental Group 14 exhibited the smallest
 6 temperature rise in the return section. At this point, the cover material had the lowest thermal conductivity, the pipe material
 7 had the highest thermal conductivity, and yet the return section experienced the smallest temperature rise. This suggests that
 8 the impact of the surface cover material on pipe heat exchange is greater than that of the pipe material.

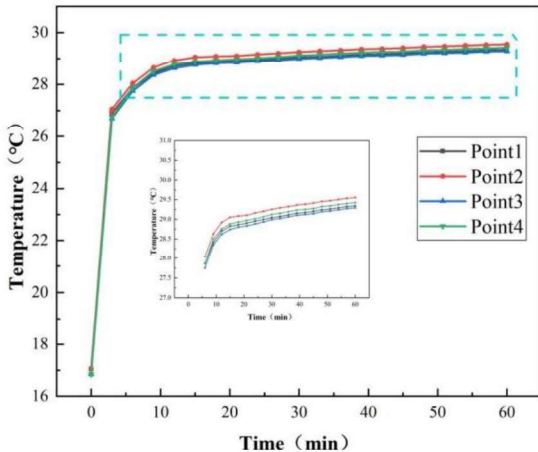
9 As shown in Fig. 11(c), after 1 hour of operation, the temperatures at points 1, 2, 3, and 4 increased from 17.05 °C,
 10 17.05 °C, 16.85 °C, and 16.85 °C to column 16 of Table 6. While Experimental Group 15 has a deeper water supply section
 11 and uses PA6 as the pipe material, its temperature rise is higher than that of Experimental Group 14 because the surface
 12 cover material, tuff, promotes better heat exchange with the pipe. It can be observed that in Experimental Group 15, the
 13 temperature rise is more pronounced within the first 15 minutes, with a delay of 3 minutes compared to the previous 12
 14 minutes. This delay is due to the increased burial depth, which causes delayed heating of the surface temperature of the
 15 cover material. During this period, the tuff cover material facilitates the downward transfer of heat, albeit with some delay.



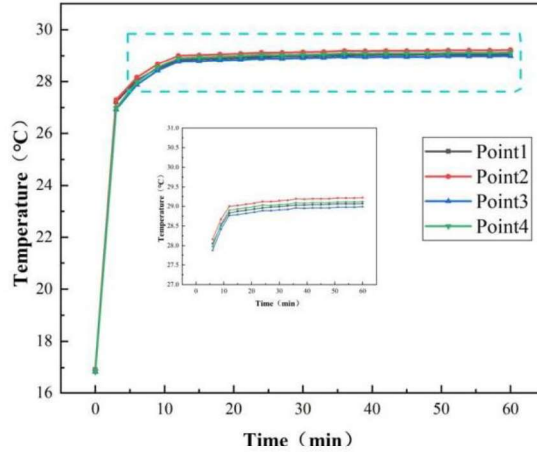
(a) Group 13: dolomite gravel, 2.0 cm, PE, 3 L/min



(b) Group 14: soil sand, 3.5 cm, PVC, 2 L/min



(c) Group 15: limestone gravel, 5.0 cm, PA6, 4 L/min



(d) Group 16: sandstone gravel, 6.5cm, HDPE, 5L/min

Fig. 11 Horizontal manifold Temperature Sensor Change at 50 °C Surface Temperature

16 As depicted in Fig. 11(d), at points 1, 2, 3, and 4, the temperatures increased from 16.93 °C, 16.93 °C, 16.85 °C, and
 17 16.85 °C to column 17 of Table 6. The temperature rise was significant within the first 12 minutes, and there was minimal
 18 temperature change after 12 minutes. Experimental Group 16 exhibited the same temperature rise in the return section as
 19 Experimental Group 15. In this case, even though the thermal conductivity of the cover material, sandstone, was lower than

1 that of tuff in Experimental Group 15, the combined effects of pipe materials and pipe flow rate in Experimental Group 16
 2 resulted in the same temperature rise in the return section as Experimental Group 15. Compared to Experimental Groups 13,
 3 14, and 15, the temperature rise was not significant after 12 minutes in Experimental Group 16, primarily due to the deeper
 4 burial depth and the lower thermal conductivity of the sandstone cover material. At this point, the U-shaped heat exchanger
 5 experienced the least reduction in temperature due to the minimal temperature rise in the water supply section.

6 *3.2 Horizontal manifold supply and return section heat-transfer rate*

7 The heat-transfer rate reflects the strength of the heat exchange between the pipe and the gravel. The heat-transfer rate
 8 is calculated as follows. Negative results of the calculation indicate a decrease in the exothermic temperature of the pipe.

9
$$Q = c_f \rho_f q_v (t_1 - t_2)$$

10 Where Q is the heat-transfer rate (W), c_f is the specific heat capacity of the fluid (J/(kg·°C)), ρ_f is the density of the
 11 fluid (kg/m³), q_v is the volumetric flow rate of the fluid (m³/s), t_1 is the temperature of the fluid at the outlet (°C), and
 12 t_2 is the temperature of the fluid at the inlet (°C).

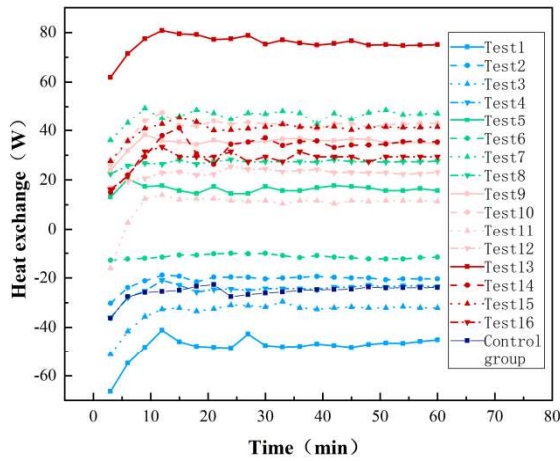
13 As shown in Fig. 12, under different operating conditions, the heat-transfer rate of the water supply and return sections
 14 of the horizontal manifold varies. To investigate how changes in the burial method of the horizontal manifold affect the
 15 heat-transfer rate in the water supply and return sections, an L16 (4⁵) orthogonal experiment was conducted. The
 16 heat-transfer rate for the water supply section of the horizontal collector pipe for experimental groups 1 - 16 can be seen in
 17 the third row of Table 7 after the experiment was stabilised. The heat-transfer rates for the return section of the horizontal
 18 manifold can be found in the fifth row of Table 7.

19 Table 7 Change in heat-transfer rate for buried pipes

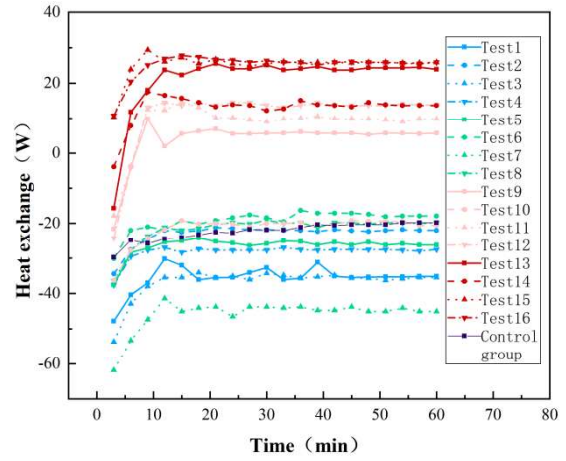
Heat-transfer rate (W)	Experimental group																Control group
	1	2	3	4	5	6	7	8	9	10	11	12	13	14	15	16	
Supply	-45.1	-19.6	-31.4	-23.5	15.7	-11.8	47.0	27.4	29.4	43.1	11.8	23.5	74.5	35.3	41.2	29.4	-23.5
U-tube	-35.3	-39.2	-37.2	-39.2	-43.1	-39.2	-54.9	-45.1	-49.0	-52.9	-41.2	-43.1	-62.7	-47.0	-51.0	-45.1	-41.2
Return	-35.3	-21.6	-35.3	-27.4	-25.5	-17.6	-45.1	-19.6	5.9	-21.6	9.8	13.7	23.5	13.7	25.5	25.5	-19.6

20 When the surface temperature increases from 20 °C to 50 °C, the temperature in the horizontal manifold changes from
 21 initially decreasing to increasing, indicating that surface temperature has a significant impact on the temperature changes in
 22 the water supply and return pipes. Experimental Group 13 in the water supply section and Experimental Group 16 in the
 23 return section have the highest heat-transfer rate, at 74.5 W and 25.5 W, respectively. Under these conditions, excessive
 24 temperature rise in the water supply and return sections can offset the cold obtained by the U-shaped heat exchanger from
 25 the geotechnical body, which is not conducive to the overall heat exchange in the system. Therefore, when the surface
 26 temperature is high, to prevent temperature rise in the water supply and return sections, it is advisable to use cover materials
 27 and piping materials with low thermal conductivity while increasing burial depth and pipe flow rate.

28 The heat exchange between Experimental Group 1 in the water supply section and Experimental Group 7 in the return
 29 section is both -45.1 W. In this condition, both the water supply and return sections, as well as the U-shaped heat exchanger,
 30 receive cold from the geotechnical body, thereby improving the heat exchange efficiency of the system under the most
 31 favorable conditions. Therefore, when the surface temperature is low, increasing burial depth, reducing pipe flow rate, and
 32 using cover materials and piping materials with higher thermal conductivity should be considered to enable the water supply
 33 and return sections to obtain more cold.



(a) Heat-transfer rate in the water supply section



(b) Heat-transfer rate in return section

Fig. 12 Horizontal manifold supply and return section heat-transfer rate

3.3 Influence of horizontal manifold on U-shaped heat transfer

Due to the different heat-transfer rate of the water supply sections in the horizontal manifold, the heat extracted by the U-shaped heat exchanger from the geotechnical body also varies, and this variation is depicted in Fig. 13. From the figure, it is evident that the maximum heat exchange occurs at the outset of system operation, gradually decreasing and eventually stabilizing. The heat-transfer rates of the U-type heat exchangers for orthogonal tests 1 to 16 after the system has stabilised in operation are shown in the fourth row of Table 7.

As the surface temperature increases, it leads to an elevation in the water supply section's temperature. This increase in the water supply section's temperature intensifies the heat exchange between the U-shaped heat exchanger and the geotechnical body. Experimental group 13 exhibits the highest heat-transfer rate at 62.7 W. However, at this point, its water supply section's heat-transfer rate is 74.5 W, surpassing the heat-transfer rate of the U-shaped heat exchanger from the geotechnical body. This indicates that under these conditions, the buried pipe system not only fails to lower the water temperature but actually increases it, which is not permissible in practical projects.

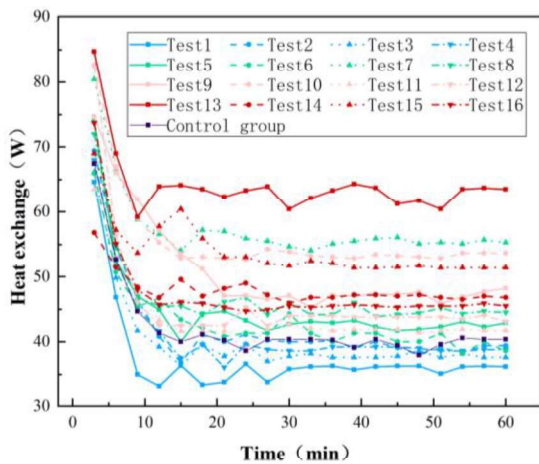


Fig. 13 U-shaped heat exchange

making it the most favorable operating condition. This is because, at this time, the surface temperature is the lowest, the piping material has the highest thermal conductivity, the surface covering material also exhibits relatively high thermal conductivity, and the water supply section is buried at the greatest depth. Conversely, as surface temperature rises, in order to prevent temperature increases in the water supply and return sections, the surface covering material and piping material

In comparison to the control group, experimental group 1, although having the lowest heat-transfer rate for the U-shaped heat exchanger at 35.3 W, experiences a temperature reduction of 0.23 °C in its water supply section and 0.18 °C in its return section. The water outlet temperature from the buried pipe system is 0.59 °C lower than the incoming water temperature. The combined heat-transfer rate of the water supply and return sections in experimental group 1, when added to the U-shaped heat exchanger's capacity, is the highest at 115.6 W. The overall heat transfer of the system was 31.3 W higher than that of the control group, resulting in a 37 % increase in overall heat transfer performance. Under these conditions, the overall heat-transfer rate of the system reaches its peak,

1 should be replaced with materials of greater thermal conductivity, thus validating the hypothesis in section 3.2. It can be
2 concluded that surface temperature has a more significant impact on the heat exchange in the water supply and return
3 sections compared to surface covering and piping materials.

4 Under the most favourable operating conditions, the U-shaped heat exchanger has the lowest heat-transfer rate, but the
5 overall heat-transfer rate of the system is the highest. On the contrary, under the most unfavourable working conditions, the
6 U-shaped heat-transfer rate is the highest, but the overall heat-transfer rate of the system is the lowest, and there is an
7 anomaly that the temperature of the return section is higher than that of the supply section. This indicates that even if the
8 efficiency of the individual components of the buried pipe is not optimal, the performance of the overall system can still be
9 optimised through appropriate system design and configuration. Therefore, we emphasise that when designing and
10 optimising buried pipes, it is important to consider not only the efficiency of individual components, but also the synergy
11 between components, in order to maximise the efficiency of the overall system.

12 **4 Discussion**

13 *4.1 Values of temperature rise in the water supply section*

14 Based on the analysis above, it's evident that temperature changes occur in both the supply and return sections of the
15 horizontal manifold under various experimental conditions. Since the return section consistently has a greater burial depth
16 than the supply section, it is less affected by ground temperature. When the temperature of the supply section decreases, the
17 temperature of the return section must also decrease, while an increase in the supply section's temperature may lead to a
18 decrease in the return section's temperature. Consequently, the supply section exerts the most significant influence on the
19 overall heat transfer of the system. To maximize the system's overall heat transfer, it is necessary to reduce the temperature
20 of the supply section. Therefore, this analysis focuses on the temperature changes in the water supply section of the
21 horizontal manifold.

22 During the 1 hour experiment, the temperatures at points 1 and 2 become relatively stable. The temperature variation
23 between point 1 and point 2 is presented in Table 6, Row 7. Examining the table, it becomes apparent that the water supply
24 section's temperature in experimental group 13 exhibits the highest increase, while in experimental group 1, the water
25 supply section's temperature decreases the most. This suggests that under these conditions, experimental group 13 has the
26 most pronounced impact on the heat transfer within the horizontal manifold, as its supply section experiences the greatest
27 temperature rise, whereas experimental group 1 records the most substantial temperature reduction in its supply section.
28 Conversely, experimental group 6 and experimental group 11 show the smallest temperature changes in their supply sections,
29 indicating that under these conditions, heat transfer within the horizontal manifold is minimal. Under these circumstances,
30 the overall heat exchange of the system predominantly arises from the heat exchange between the U-shaped heat exchanger
31 and the geotechnical body.

32 Based on Table 7, the optimal configurations for the four scenarios, considering the horizontal manifold placement at
33 ground temperatures ranging from 20 °C to 50 °C, are as follows: Experimental Group 1, Experimental Group 6,
34 Experimental Group 11, and Experimental Group 16. Comparing the best-case scenarios with the worst-case scenarios for
35 water supply section heat transfer, heat losses can be reduced by 25.5 W, 58.8 W, 31.3 W, and 45.1 W, respectively.

36 *4.2 Analysis of extreme variations in temperature*

37 A polar analysis of the temperature changes in the water supply section of the horizontal manifold obtained from the
38 orthogonal test is shown in Table 8. $K_1 - K_4$ represent the sum of the temperature changes in the water supply section of the
39 five factors at the four levels, respectively. For example, these five numbers in the K_1 row are the sum of the temperature
40 changes in the water supply section corresponding to the factors surface temperature, surface cover material, water supply
41 section burial depth, piping material, and piping flow rate. In this case, the factor surface temperature 20 °C (first column),
42 which is arranged at the first level in experimental groups 1, 2, 3, and 4, corresponds to water supply section temperature
43 changes of - 0.23, - 0.10, - 0.16, and - 0.12, respectively, and the sum of which is - 0.61, which is recorded in the first
44 column of the K_1 row.

1 The difference obtained by subtracting the minimum from the maximum of the four numbers $\kappa_1 - \kappa_4$ in the same
 2 column is the extreme difference. Here it was calculated that the first column, i.e., the factor surface temperature, had the
 3 highest extreme difference, which indicates that the level of the factor had the greatest effect on the experiment when it was
 4 changed. The values corresponding to the four levels of surface temperature are -0.153, -0.100, 0.138, and 0.230, and the
 5 value corresponding to the first level, -0.153, is the smallest, so it is best to take its first level, i.e., a surface temperature of
 6 20 °C. The value 0.230 corresponding to the fourth level is the largest, so its fourth level is taken as the worst, i.e., surface
 7 temperature 50 °C. Similarly, the best and worst solutions for the other factors can be derived.

8 **Table 8** Orthogonal test polar analysis

Experimental group	Influential factors					Temperature change of water supply section °C
	Surface temperature °C	surface covering	Depth of water supply section cm	Piping materials	Pipe flow rate L/min	
1	20	Dolomite gravel	6.5	PVC	4	- 0.23
2	20	Soil sand	5.0	PE	5	- 0.10
3	20	Limestone gravel	3.5	HDPE	3	- 0.16
4	20	Sandstone gravel	2.0	PA6	2	- 0.12
5	30	Dolomite gravel	5.0	HDPE	2	0.08
6	30	Soil sand	6.5	PA6	3	- 0.06
7	30	Limestone gravel	2.0	PVC	5	0.24
8	30	Sandstone gravel	3.5	PE	4	0.14
9	40	Dolomite gravel	3.5	PA6	5	0.15
10	40	Soil sand	2.0	HDPE	4	0.22
11	40	Limestone gravel	6.5	PE	2	0.06
12	40	Sandstone gravel	5.0	PVC	3	0.12
13	50	Dolomite gravel	2.0	PE	3	0.38
14	50	Soil sand	3.5	PVC	2	0.18
15	50	Limestone gravel	5.0	PA6	4	0.21
16	50	Sandstone gravel	6.5	HDPE	5	0.15
K ₁	- 0.61	0.38	- 0.08	0.31	0.34	
K ₂	0.40	0.24	0.31	0.48	0.44	
K ₃	0.55	0.35	0.30	0.29	0.28	
K ₄	0.92	0.29	0.72	0.18	0.20	
$\kappa_1 \left(= \frac{K_1}{4} \right)$	- 0.153	0.095	- 0.020	0.078	0.085	
$\kappa_2 \left(= \frac{K_2}{4} \right)$	0.100	0.060	0.078	0.120	0.110	
$\kappa_3 \left(= \frac{K_3}{4} \right)$	0.138	0.088	0.075	0.073	0.070	
$\kappa_4 \left(= \frac{K_4}{4} \right)$	0.230	0.073	0.180	0.045	0.050	
extremely poor	0.383	0.035	0.200	0.075	0.060	
Poor Solution	50	Dolomite gravel	2.0	PE	5	
Excellent	20	Soil sand	6.5	PA6	2	

As can be seen from Table 8, the five factors of surface temperature, surface covering material, water supply section burial depth, pipe material and pipe flow rate have the following order of influence on the temperature change of the water supply section of the horizontal manifold: surface temperature > water supply section burial depth > pipe material > pipe flow rate > surface covering material. The worst scenario is only different in pipe flow rate compared to experiment 13, which is indeed the highest temperature rise scenario for the water supply section. The best scenario is: 20 °C, soil sand, 6.5 cm, PA6, 2 L/min. In the setting of the parameters of the optimal scheme, the lowest surface temperature can reduce the temperature of the water supply section, and the lowest rock temperature at the deepest burial of the water supply section is favorable for heat exchange. The use of the pipe material PA6 with low thermal conductivity and the cover material soil can effectively reduce the surface temperature impact on the water supply section and the thermal short-circuit in the return section. It can be determined that this solution is the optimal solution.

According to the similar parameters in Table 2, 6.5 cm indicates a burial depth of 1.3 m. Therefore, the optimal solution is applied to the actual project, i.e.: when the horizontal manifold is laid out in the underground garage, the water supply section is buried at a depth of 1.3 m, the water return section is buried at a depth of 1.6 m, backfilling is carried out using soil sand, the pipe is made of PA6 material, and the flow rate is selected to be 2 L/min.

4.3 Reduction of heat loss from horizontal manifold

The five factors that influence heat exchange in the horizontal manifold are: surface temperature, water supply section burial depth, pipe material, surface covering material, and pipe flow rate. Surface temperatures are set at 20 °C, 30 °C, 40 °C, and 50 °C, allowing the experimental conclusions to be applied to scenarios where horizontal manifolds are installed in underground parking lots, lawns, squares, and roads. However, in actual engineering, ground temperatures constantly fluctuate, while the experimental conclusions are based on constant temperatures, resulting in potential errors when applying the experimental results to real-world projects.

In this study, the burial method for horizontal manifold differs from the traditional approach. The new burial method aims to prevent heat loss while maintaining the burial depth of the return section unchanged, only altering the burial depth of the water supply section. Experimental data confirm that this new burial method effectively reduces heat loss from the horizontal manifold. The thermal conductivity of both pipe materials and surface covering materials directly impacts heat exchange in the horizontal manifold. Furthermore, the influence of pipe materials on heat exchange in the horizontal manifold is greater than that of surface covering materials. Therefore, it is advisable to prioritize reducing heat loss caused by pipe materials.

One potential approach is to use high thermal conductivity pipe materials in the return section to enhance heat exchange while employing low thermal conductivity pipe materials in the water supply section to mitigate heat exchange. However, it's important to note that using different materials for connecting horizontal manifold may introduce the risk of leaks. To further minimize heat loss, it is possible to select surface covering materials with appropriate thermal conductivity based on the heat exchange requirements of the water supply and return sections. However, the economic feasibility of these surface covering materials should also be taken into consideration.

Summer studies have found that changing the horizontal manifold arrangement can significantly increase the heat-transfer rate and efficiency of the system. For winter heating, this finding also applies, as changing the supply and return depth and arrangement can also affect the efficiency of heat exchange. However, the lower ground temperatures in winter compared to summer may affect the degree of improvement in heat exchange efficiency. Therefore, although the principles of optimisation of the arrangement are similar, the exact effect and optimum configuration may differ. Where the efficiency of individual components in the buried pipe section is not optimal, the overall system can still achieve optimal performance through proper configuration. This principle also applies in winter, as the overall performance of the system, both for cooling and heating, depends on the synergy between the components. Rank the importance of the main influencing factors. In winter, these factors may still be important, but their relative degree of influence may change. Optimisation methods for different scenarios provided in the summer can be used as a reference for the winter to adapt to different

1 thermal demands and external temperature conditions.

2 **5 Conclusion**

3 In this study, L16 (4⁵) orthogonal tests are carried out on five main factors affecting the heat exchange of horizontal
4 manifold after changing the way of burying horizontal manifold for GSHP. The change of heat-transfer rate of horizontal
5 manifold under different scenarios is analyzed, and the change of heat-transfer rate of manifold affects the heat exchange of
6 U-shaped heat exchanger. The degree of influence of five factors on the heat exchange of horizontal manifold is analyzed
7 using extreme variance and the optimal and worst scenarios for buried pipes are obtained. Finally, the optimal scheme of
8 buried pipe for horizontal manifold arrangement in different scenarios is provided. The main conclusions are as follows:

9 (1) When the ground temperature is 20 °C, changing the horizontal manifold arrangement (with varying burial depths
10 for supply and return, supplying water from the near-ground side and returning water from the far-ground side) can increase
11 the overall system heat exchange by 31.3 W and improve the heat exchange efficiency of the buried pipe system by 37 %.

12 (2) The efficiency of individual components of the buried pipe system is not optimal, and the performance of the
13 overall system can still be optimised through reasonable configuration. It shows that in practical engineering, the design and
14 optimisation of buried pipes should not only consider the efficiency of individual components, but also pay more attention
15 to the synergistic effect between the components.

16 (3) The degree of influence of the five factors on the horizontal manifold is as follows: surface temperature > water
17 supply section depth > pipe material > pipe flow rate > surface covering material.

18 (4) In summer working conditions, when the horizontal manifold is arranged in different scenes in the building
19 underground garage, lawn, square, asphalt pavement, applied to the actual project, the water supply section burial depth are
20 1.3 m, the pipe material is suitable to choose PA6, PA6, PE, HDPE, the pipeline flow rate is chosen 2 L/min, 3 L/min, 2
21 L/min, 5 L/min, and the cover material is chosen soil sand, soil sand, grey rock gravel, sandstone gravel.

22 This study provides insights into the heat exchange characteristics of horizontal manifolds with some limitations. There
23 are discrepancies between our experimental model in terms of simulating the ground temperature and the surface covering
24 material and the real situation. In real-world environments, the ground temperature changes over time and the cover material
25 is usually not completely dry. These factors may affect the heat exchange performance of horizontal manifolds. In addition,
26 the research has focused on summer cooling, and studies related to winter heating have not yet been conducted. Therefore,
27 the results of this study are primarily for summer cooling conditions and may be limited in their applicability to systems
28 used for both winter heating and summer cooling. Additional research and validation is needed to determine if these
29 findings are equally applicable to winter heating conditions. The influence of these factors on the heat exchange
30 effectiveness of horizontal manifolds could be discussed in the future through more detailed experiments or numerical
31 simulations. The scope of the study is also extended to the analysis of heat exchange characteristics under winter heating
32 conditions. More accurate prediction and optimisation of horizontal manifold heat exchange systems in practical
33 applications will lead to improved efficiency and reliability.

34 **Declaration of Competing Interests**

35 The authors declare that they have no known competing financial interests or personal relationships that could have
36 appeared to influence the work reported in this paper.

37 **Acknowledgments**

38 The author would like to thank the financial support of the National Natural Science Foundation of China
39 (NO.52168013), and the Guizhou Provincial Science and Technology Projects (No. ZK [2022]151 and [2019]1102).

40
41
42

1 **References:**

- 2 [1]C.S. Hendrix, V. Koubi, J. Selby, A. Siddiqi, N. von Uexkull, Climate change and conflict, *Nature Reviews Earth &*
3 *Environment*, 4(2023) 144-148.
- 4 [2]M. Attwaters, Climate change down the road, *Nature Reviews Earth & Environment*, 4(2023) 140.
- 5 [3]H. Weeratunge, G.R. Aditya, S. Dunstall, J. de Hoog, G. Narsilio, S. Halgamuge, Feasibility and performance analysis of
6 hybrid ground source heat pump systems in fourteen cities, *ENERGY*, 234(2021) 121254.
- 7 [4]K. Li, A Special Issue on Geothermal Energy and Its Application, *Mathematical Geosciences*, 51(2019) 267-269.
- 8 [5]A. García-Gil, G. Goetzl, M.R. Kłonowski, S. Borovic, D.P. Boon, C. Abesser, M. Janza, I. Herms, E. Petitclerc, M.
9 Erlström, J. Holecek, T. Hunter, V.P. Vandeweyer, R. Cernak, M. Mejías Moreno, J. Epting, Governance of shallow
10 geothermal energy resources, *ENERGY POLICY*, 138(2020) 111283.
- 11 [6]I.A. Gondal, Prospects of shallow geothermal systems for sustainable heating and cooling of buildings, *ENERGY*, (2021)
12 1-25.
- 13 [7]A. Kapıcıoğlu, H. Esen, Economic and environmental assessment of ground source heat pump system: The case of Turkey,
14 *Sustainable Energy Technologies and Assessments*, 53(2022) 102562.
- 15 [8]Q. Mao, Y. Chen, Experimental investigation of thermal performance of a ground source heat pump system for spring
16 season, *ENERGY AND BUILDINGS*, 152(2017) 336-340.
- 17 [9]X. Zhang, E. Wang, L. Liu, C. Qi, J. Zhen, Y. Meng, Analysis of the operation performance of a hybrid solar
18 ground-source heat pump system, *ENERGY AND BUILDINGS*, 268(2022) 112218.
- 19 [10]X. Hu, R. Miao, Y. Yu, A.C. Megri, Development of a high-efficiency and cost-effective ground source heat pump system
20 for hot-climate applications, *INDOOR AND BUILT ENVIRONMENT*, 32(2022) 387-407.
- 21 [11]C. Zhang, E. Nielsen, J. Fan, S. Furbo, Thermal behavior of a combi-storage in a solar-ground source heat pump system
22 for a single-family house, *ENERGY AND BUILDINGS*, 259(2022) 111902.
- 23 [12]T. You, W. Wu, H. Yang, J. Liu, X. Li, Hybrid photovoltaic/thermal and ground source heat pump: Review and perspective,
24 *Renewable and Sustainable Energy Reviews*, 151(2021) 111569.
- 25 [13]S. Mohammadzadeh Bina, H. Fujii, S. Tsuya, H. Kosukegawa, Comparative study of hybrid ground source heat pump in
26 cooling and heating dominant climates, *ENERGY CONVERSION AND MANAGEMENT*, 252(2022) 115122.
- 27 [14]Y. Shimada, Y. Uchida, I. Takashima, S. Chotpantarat, A. Widiatmojo, S. Chokchai, P. Charusiri, H. Kurishima, K.
28 Tokimatsu, A Study on the Operational Condition of a Ground Source Heat Pump in Bangkok Based on a Field Experiment
29 and Simulation, *Energies*, 13(2020).
- 30 [15]Y. Shimada, K. Tokimatsu, T. Asawa, Y. Uchida, A. Tomigashi, H. Kurishima, Subsurface utilization as a heat sink for
31 large-scale ground source heat pump: Case study in Bangkok, Thailand, *RENEWABLE ENERGY*, 180(2021) 966-979.
- 32 [16]C. Kaneko, M. Yoshinaga, Long-term operation analysis of a ground source heat pump with an air source heat pump as an
33 auxiliary heat source in a warm region, *ENERGY AND BUILDINGS*, 289(2023) 113050.
- 34 [17]A.R. Puttige, S. Andersson, R. Östin, T. Olofsson, Modeling and optimization of hybrid ground source heat pump with
35 district heating and cooling, *ENERGY AND BUILDINGS*, 264(2022) 112065.
- 36 [18]H. Zeng, N. Diao, Z. Fang, Efficiency of vertical geothermal heat exchangers in the ground source heat pump system,
37 *Journal of Thermal Science*, 12(2003) 77-81.
- 38 [19]X. Meng, Z. Han, H. Hu, H. Zhang, X. Li, Studies on the performance of ground source heat pump affected by soil
39 freezing under groundwater seepage, *Journal of Building Engineering*, 33(2021) 101632.
- 40 [20]Z. Liu, P. Sun, S. Li, Z.J. Yu, M. El Mankibi, L. Roccamena, T. Yang, G. Zhang, Enhancing a vertical earth-to-air heat
41 exchanger system using tubular phase change material, *Journal of Cleaner Production*, 237(2019) 117763.

- 1 [21]J. Du, Z. Luo, W. Ge, Study on the simulation and optimization of the heat transfer scheme in a buried-pipe ground-source
2 heat pump, *Arabian Journal of Geosciences*, 13(2020) 505.
- 3 [22]J. Luo, H. Zhao, J. Jia, W. Xiang, J. Rohn, P. Blum, Study on operation management of borehole heat exchangers for a
4 large-scale hybrid ground source heat pump system in China, *ENERGY*, 123(2017) 340-352.
- 5 [23]J. Luo, J. Rohn, W. Xiang, D. Bertermann, P. Blum, A review of ground investigations for ground source heat pump
6 (GSHP) systems, *ENERGY AND BUILDINGS*, 117(2016) 160-175.
- 7 [24]A.A. DiCarlo, Novel seasonal enhancement of shallow ground source heat pumps, *APPLIED THERMAL*
8 *ENGINEERING*, 186(2021) 116510.
- 9 [25]X. Tian, R. Mao, P. Pei, H. Wu, H. Ma, C. Hu, Z. Zhang, Experimental study on temperature control optimization of
10 ground source heat pump horizontal headers, *ENERGY AND BUILDINGS*, 277(2022) 112541.
- 11 [26]E. Marín, A. Calderón, O. Delgado-Vasallo, Similarity theory and dimensionless numbers in heat transfer, *EUROPEAN*
12 *JOURNAL OF PHYSICS*, 30(2013) 439.
- 13 [27]L. Xinpei, W. Yanen, Y. Mingming, W. Kai, W. Yi, The study of biobinder droplet impacting on HA particle surface
14 depending on nondimensional scale similarity theory, *Frontiers in Bioengineering and Biotechnology*, 4(2016).
- 15 [28]K. Zhou, J. Mao, Y. Li, J. Xiang, Parameters optimization of borehole and internal thermal resistance for single U-tube
16 ground heat exchangers using Taguchi method, *ENERGY CONVERSION AND MANAGEMENT*, 201(2019) 112177.
- 17 [29]S.S. Mousavi Ajarostaghi, H. Javadi, S.S. Mousavi, S. Poncet, M. Pourfallah, Thermal performance of a single U-tube
18 ground heat exchanger: A parametric study, *Journal of Central South University*, 28(2021) 3580-3598.
- 19 [30]K. Zhou, J. Mao, Y. Li, Optimal Parameter Scenario of Borehole Thermal Resistance for Vertical Ground Heat Exchanger
20 Using Taguchi Method, *IOP Conference Series Earth and Environmental Science*, 495(2020) 12001.
- 21 [31]N. Makasis, G.A. Narsilio, A. Bidarmaghz, I.W. Johnston, Ground-source heat pump systems: The effect of variable pipe
22 separation in ground heat exchangers, *COMPUTERS AND GEOTECHNICS*, 100(2018) 97-109.
- 23 [32]Y. Luo, G. Xu, T. Yan, Performance evaluation and optimization design of deep ground source heat pump with
24 non-uniform internal insulation based on analytical solutions, *ENERGY AND BUILDINGS*, 229(2020) 110495.
- 25 [33]S. Su, R. Yang, L. Liu, C. Zhou, L. Shi, Study on the Influential Factors of Heat Transfer of Ground Heat Exchanger with
26 Orthogonal Test, *Iop Conference Series: Earth & Environmental Science*, 2017.
- 27 [34]C. Li, Y. Guan, Y. Feng, C. Jiang, S. Zhen, X. Su, Comparison of influencing factors and level optimization for heating
28 through deep-buried pipe based on Taguchi method, *GEO THERMICS*, 91(2021) 102045.
- 29 [35]S.N. Ahmad, O. Prakash, Optimization of ground heat exchanger of the ground source heat pump system based on
30 exergetic analysis using Taguchi technique, *ARCHIVE Proceedings of the Institution of Mechanical Engineers Part C Journal*
31 *of Mechanical Engineering Science 1989-1996 (vols 203-210)*, (2021) 2141052594.
- 32 [36]Y. Liu, Y. Li, G. Jiang, Orthogonal experiment on performance of mortar made with dune sand, *CONSTRUCTION AND*
33 *BUILDING MATERIALS*, 264(2020) 120254.
- 34 [37]D. Liu, W. Zhang, Y. Tang, Y. Jian, Y. Lai, Orthogonal Experimental Study on Concrete Properties of Machine-Made Tuff
35 Sand, *Materials*, 'Vol.' 15, 2022.
- 36 [38]Y. Wang, Z. Quan, Y. Zhao, L. Wang, H. Jing, Operation mode performance and optimization of a novel coupled air and
37 ground source heat pump system with energy storage: Case study of a hotel building, *RENEWABLE ENERGY*, 201(2022)
38 889-903.
- 39 [39]X.Q. Zhai, X.W. Cheng, R.Z. Wang, Heating and cooling performance of a minitype ground source heat pump system,
40 *APPLIED THERMAL ENGINEERING*, 111(2017) 1366-1370.
- 41 [40]T. Aprianti, E. Tan, C. Diu, B. Sprivulis, G. Ryan, K. Srinivasan, H.T. Chua, A comparison of ground and air source heat
42 pump performance for domestic applications: A case study in Perth, Australia, *INTERNATIONAL JOURNAL OF ENERGY*

- 1 RESEARCH, 45(2021) 20686-20699.
- 2 [41]M. Sim, D. Suh, A heuristic solution and multi-objective optimization model for life-cycle cost analysis of solar
3 PV/GSHP system: A case study of campus residential building in Korea, Sustainable Energy Technologies and Assessments,
4 47(2021) 101490.
- 5 [42]D.A. Rodriguez-Alejandro, A. Olivares-Arriaga, J.A. Moctezuma-Hernandez, A. Zaleta-Aguilar, J.A. Alfaro-Ayala, S.
6 Cano-Andrade, Comprehensive analysis of a vertical ground-source heat pump for residential use in Mexico,
7 GEOTHERMICS, 99(2022) 102300.
- 8 [43]R.J. Moffat, Describing the uncertainties in experimental results, EXPERIMENTAL THERMAL AND FLUID SCIENCE,
9 1(1988) 3-17.
- 10 [44]B. Du, Y. He, Y. Qiu, Q. Liang, Y. Zhou, Investigation on heat transfer characteristics of molten salt in a shell-and-tube
11 heat exchanger, INTERNATIONAL COMMUNICATIONS IN HEAT AND MASS TRANSFER, 96(2018) 61-68.